Effects of Pressure on the Transport of Ions through Rotating Helium II*

B. E. SPRINGETT
Department of Physics and Institute for the Study of Metals, The University of Chicago, Chicago, Illinois
(Received 8 September 1966)

This paper describes measurements of the cross section for capture of negative ions by vortex lines in He II and of the mobility of the negative ion, as a function of both pressure and temperature. The first of these measurements is used to derive the variation of the negative-ion radius with pressure. The bubble model of the negative ion is then discussed in the light of the derived radii and an explanation of the mobility measurements is given. Certain null results on positive ions are also presented.

I. INTRODUCTION

SINCE about 1960 there have been published many reports of experiments with ions in Helium II. These experiments may be somewhat arbitrarily divided into those performed above 1°K and those below 1°K. The former group consists of mobility measurements in a stationary frame[1–3] and studies of interactions with vortex structure in a rotating frame.[4–6] The latter group consists again of mobility measurements[1] and studies of hot ions and vortex rings created by such ions in a stationary frame.[7–9] In this paper we are concerned with the interaction of negative ions with vortex structure in a rotating frame under the application of pressure. The purpose of these experiments was twofold: first, to extend the measurements of Ref. 5 to include pressure variation, and, second, to attempt to get further experimental evidence on the nature of the negative ion.

A vortex line presents a width σ_0 to a beam of ions which is typically of the order of 10^{-5} cm. An ion approaching closer than a distance σ_0 to a line is trapped with a certain lifetime. A formalization of these ideas can be obtained by treating the ion as a Brownian particle. It turns out that σ_0 may be written as $(2\pi kT/e\epsilon)g(e\epsilon d/kT)$, where d is some length characteristic of the ion-vortex system, ϵ is the electric field, T is the temperature, and g is a complicated function of these variables. The lifetime of an ion trapped on a line may be written as $\tau(\epsilon,T)\exp(U/kT)$, where U is the depth of the potential well in which the ion is trapped and $\tau(\epsilon,T)$ is a characteristic time of the ion-vortex system. The details of this theory have been worked out by Donnelly and Roberts.[10] This paper is concerned mainly with the trapped lifetime because this yields the most information about the ion. The theory predicts that the lifetime will be influenced in the following two ways. First, it will increase as the superfluid density ρ_s increases; second, it will increase as the ion radius R increases. The effect of pressure on the superfluid density may be calculated to fair accuracy from the Landau model using the neutron data of Henshaw and Woods.[11] The bubble model of the negative ion, as enumerated by several authors[12–16] and so far substantiated directly only by the experiment of Levine and Sanders,[17] predicts a decrease of the ion radius with increasing pressure. We conclude that the observations presented in this paper result from changes in both the He II and the negative ion. The sechanges are competing effects in the temperature and pressure region we explored. The theory may be fitted to the cross-section data, because the only totally unknown quantity is R. A check on the values of radii so obtained was made by comparing the experimental variation with pressure of the negative-ion mobility μ_- with a theoretical estimate of μ_-. Also, the bubble model of the negative ion was examined in the light of the present experimental values of R.

Positive ions were examined under the same experimental conditions, and from these results a conclusion as to the size of the positive ions is drawn.

* Research supported by the National Science Foundation under Grant No. GP-5302, and by the U. S. Air Force Office of Scientific Research under Grant No. AF-AFOSR 785-65. This research has also benefitted from the use of facilities provided by the Advanced Research Projects Agency for materials research at the University of Chicago.

[1] F. Reif and L. Meyer, Phys. Rev. **119**, 1164 (1960).
[2] F. Scaramuzzi, Comitato Nazionale per l'Energia Nucleare, Laboratori Nazionale di Frascati, nota interna: n.225 (unpublished).
[3] L. Meyer and F. Reif, Phys. Rev. **123**, 727 (1961).
[4] G. Careri, W. D. McCormick, and F. Scaramuzzi, Phys. Letters **1**, 61 (1962).
[5] B. E. Springett, D. J. Tanner, and R. J. Donnelly, Phys. Rev. Letters **14**, 585 (1965).
[6] R. L. Douglass, Phys. Rev. Letters **13**, 791 (1964); Phys. Rev. **141**, 192 (1966).
[7] G. Careri, S. Consolo, P. Mazzoldi, and M. Santini, Phys. Rev. Letters **15**, 932 (1965).
[8] G. W. Rayfield and F. Reif, Phys. Rev. **136**, 1194 (1964).
[9] L. Bruschi, B. Maraviglia, and P. Mazzoldi, Phys. Rev. **143**, 84 (1966).
[10] R. J. Donnelly and P. H. Roberts, in *Superfluid Helium*, edited by J. F. Allen, (Academic Press Inc., New York, 1966), p. 103.
[11] D. G. Henshaw and A. D. B. Woods, in *Proceedings of the Seventh International Conference on Low-Temperature Physics, 1960* (University of Toronto Press, Toronto, 1961), p. 539.
[12] R. A. Ferrel, Phys. Rev. **108**, 167 (1957).
[13] C. G. Kuper, Phys. Rev. **122**, 1007 (1961).
[14] J. Jortner, N. R. Kestner, S. A. Rice, and M. H. Cohen, J. Chem. Phys. **43**, 2614 (1965).
[15] K. Hiroike, N. R. Kestner, S. A. Rice, and J. Jortner, J. Chem. Phys. **43**, 2625 (1965).
[16] M. H. Cohen, B. E. Springett, and J. Jortner, Phys. Rev. (to be published).
[17] J. Levine and T. M. Sanders, Phys. Rev. Letters **8**, 159 (1962).

Finally, the relevance of the results of these experiments to other experiments recently published is discussed.

II. APPARATUS AND METHODS

A. Apparatus

The system in which the measurements were made consists of a conventional helium Dewar in which a brass can is immersed. Helium is condensed into this can via 18 in. of 30-mil stainless-steel capillary tubing. When the can is filled, the desired pressure is applied to the top end of the capillary from a small tank of helium via a pressure regulator. A Heise gauge accurate to $\frac{1}{4}$ psi is connected to this pressure line. Inside the can is a grid assembly together with a 56-Ω Allen-Bradley 0.1-W carbon resistor for temperature measurement. Outside the can is a 90 Ω heater for temperature regulation. Details of the can and its contents are shown in Fig. 1.

The ion current is generated by α particles from a 29 μCiAm^{241} source; the kind of ion transmitted through the helium is determined by the potential across SG_1. The distance L between G_1 and G_2 is 2.86 cm and is the operative length of the grid assembly, i.e., generally speaking, only the potential across G_1G_2 is varied in these experiments. The function of G_2 is simply to shield the collector C from voltage changes G_1. Of course, in analyzing the raw data, small corrections have to be made for the distance $SG_1+G_2C=0.24$ cm.

The signal on C is measured with a Cary 31-V vibrating reed electrometer. The signal from this electrometer is fed into a voltage-to-frequency converter. A dc output is also taken from the electrometer so that the signal can be continuously monitored. The input signal to the Cary is typically of the order of 10^{-12} A cm^{-2}.

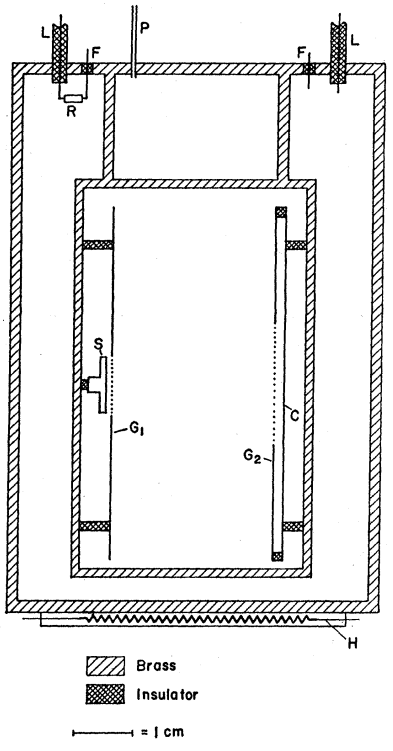

FIG. 1. Cross section of experimental chamber: C, collector; F, electrical feed throughs, 9 in all; G_1, G_2 are 40 mesh grids; H, 90-Ω heater; L, stainless-steel coaxial cables, 3 in all; P, 30-mil stainless-steel condensing line; R, 56-Ω Allen-Bradley carbon resistor; S, 29-μ CiAm^{241} α source. The transverse dimensions are SG_1 =0.08 cm, G_1G_2 =2.86 cm, G_2C =0.16 cm.

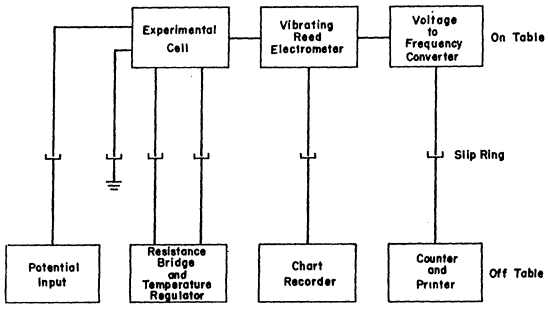

FIG. 2. Arrangement of the electrical measuring system.

All the equipment described above is mounted on a 42-in.-diam turntable which can be rotated at speeds up to 90 rpm. The pumping line to the Dewar is via a 4-in.-i.d. rotating seal. The pumping system consists of a mechanical pump and a booster diffusion pump. The lowest temperature that can be reached with the system is 0.96°K.

Voltages are led to the apparatus through mercury slip-rings; the signal is taken from the apparatus in the same manner. Details of the electrical system are shown in Fig. 2.

B. Trapping Cross-Section Measurements

The method of measuring cross sections has already been described.[5,18] Suffice it to say that we measure the current transmitted transverse to the axis of rotation as a function of angular velocity for pressures up to 20 atm and fit the equation

$$I=I_0\exp(-2mh^{-1}L\sigma\Omega), \quad (1)$$

where m is the mass of a helium atom and Ω is the angular velocity, to find the experimental cross section or capture width σ. Here $2mh^{-1}\Omega$ is the density of vortex lines/cm^2, and L is the distance traversed by the ion beam. In Figs. 3 and 4 we display the results of such measurements.

The effect of the lifetime becoming shorter than some vertical transit time is seen to be quite dramatic, and it is because of this that ion radii can be extracted from the data fairly readily. The electric field is the same in all cases shown in Figs. 3 and 4, being nominally 20 V cm^{-1}.

C. Mobility Measurements

The mobility is found by measuring the ion transit time across the distance L. This is done by applying a

[18] D. J. Tanner, Phys. Rev. 152, 121 (1966).

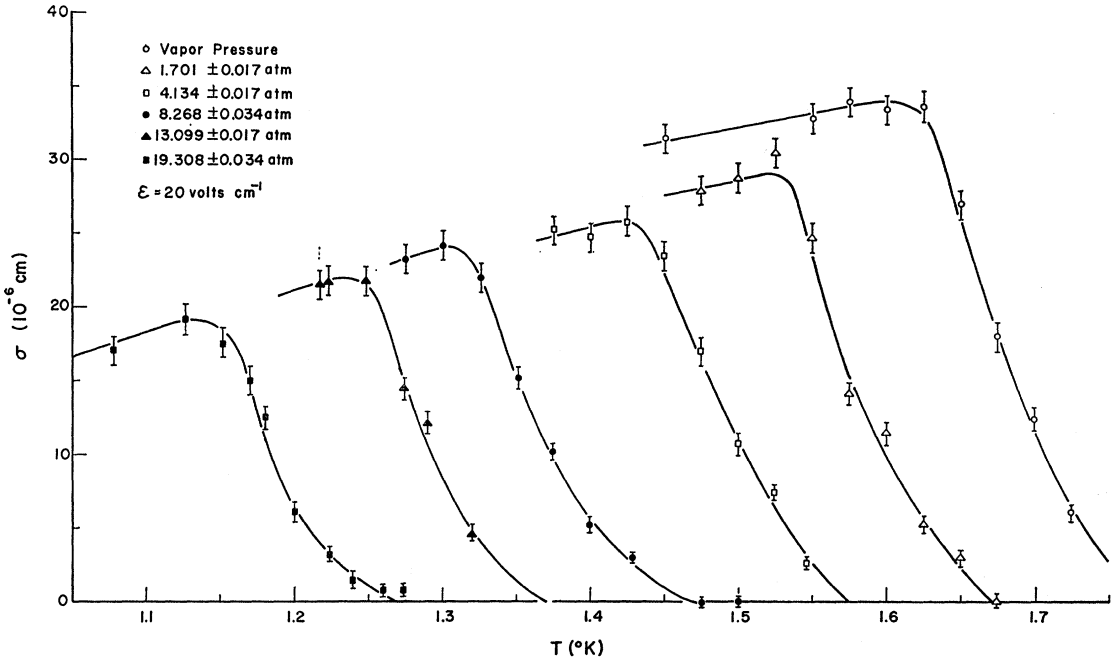

FIG. 3. Cross section versus temperature for several pressures.

square wave across G_1G_2 and plotting the current collected as a function of frequency. The current goes to zero linearly as the frequency ν is increased. The transit time is then $(2\nu_c)^{-1}$, where ν_c is the cutoff frequency. It was found that sharper cutoffs were obtained by arranging the potential on G_2 so that the forward half of the square-wave amplitude V_F was less than the reverse half V_R. The reason is presumably that such an arrangement eliminates residual space-charge effects.

The collected current then is given by

$$I = I_0(\tfrac{1}{2} - L^2\nu/\mu V_F), \tag{2}$$

where μ is the mobility in units of cm^2 sec^{-1} V^{-1}. As

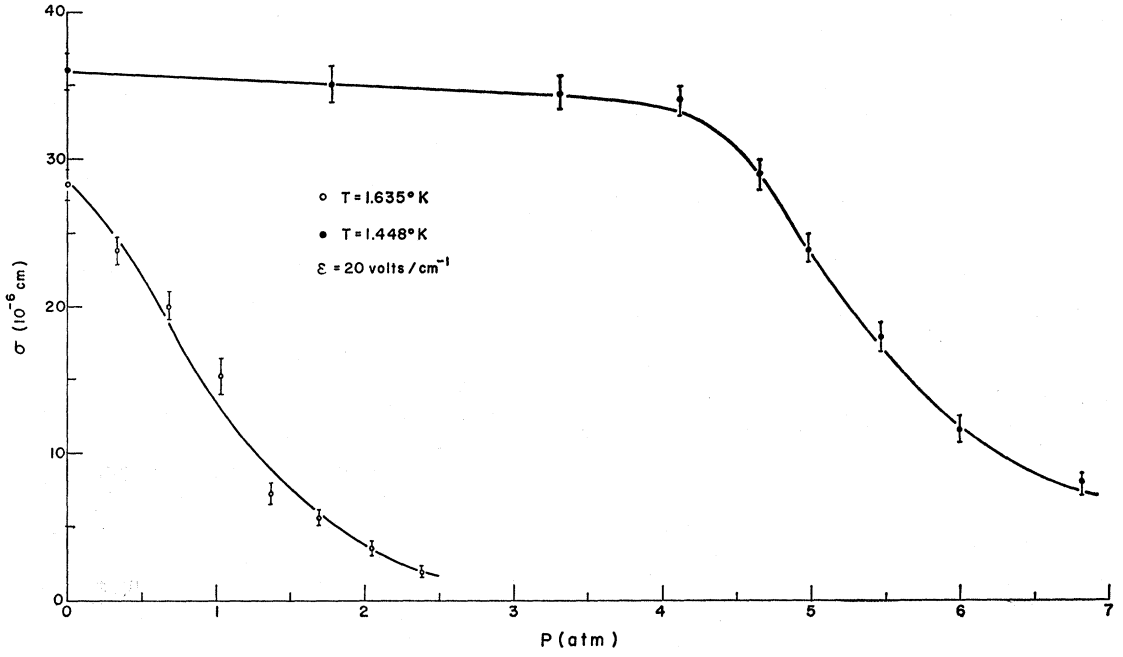

FIG. 4. Cross section versus pressure for two temperatures.

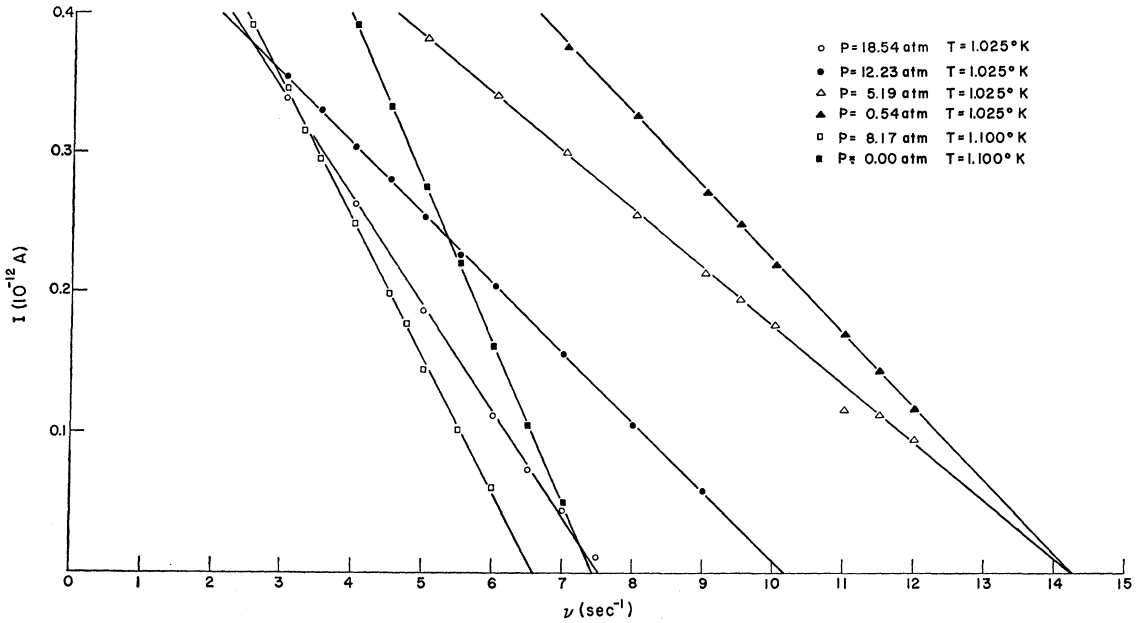

FIG. 5. Examples of current-versus-frequency measurements used in deriving μ_-.

can be seen, $I=0$ when $\nu=\nu_c=\mu V_F/2L^2$. Examples of the variation of current with frequency are shown in Fig. 5. Because of the large value of L, measurements of the mobility much above 1.1°K could not be obtained because the signal-to-noise ratio became prohibitively small.

D. Sources of Error

Temperature, pressure, angular velocity, voltages, and square-wave frequency were all measured to better than $\pm 0.2\%$. The single, largest source of error comes from measuring current. The operating currents are of the order of 10^{-12} A, and there are many sources of noise, some of which give rise to displacements in the zero of current. The purpose of the voltage-to-frequency converter was to achieve some signal averaging without resorting to integrating circuits, which obscure details of response times. Figure 5 shows that this averaging process is quite successful, for the cutoff frequency can be measured to $\pm 1\frac{1}{2}\%$ upon making a straight-line fit to the data. Cross-section measurements depend for their accuracy on the measurement of the slope of a log-linear plot of average current versus angular velocity. Because of the way in which the cross section varies with temperature, temperature stability is very important for good measurements. Under the best conditions σ was measured to $\pm 5\%$.

III. DERIVATION OF NEGATIVE-ION RADII

First, it must be pointed out that it is likely that the value found for the negative-ion radius depends on the way in which it is measured. The present determination depends on the interaction of the ion with a vortex line. Second, this determination depends on a knowledge of the variation with pressure of both the free-ion mobility and the superfluid density. Third, the ion is viewed as a Brownian particle, and for this to be true we must have $T>1$°K and the depth of the well in which the ion is trapped, $U\gg kT$. Both of these conditions hold for the present experiments. On solving the Fokker-Planck equation, Donnelly and Roberts[10] find the probability of escape of an ion from a potential well to be

$$p=(\omega_A S_A/2\pi\omega_C S_C)[(\omega_C^2/M+\beta^2/4)^{1/2}-\tfrac{1}{2}\beta]\times\exp(-U/kT). \quad (3)$$

Appendix A gives an explanation of (3) and gives details of the calculation of the various quantities involved, except for ρ_s and μ_-. The variation of these last two quantities with pressure is dealt with in Appendix B.

Once an ion is trapped on a line, it moves along the line under some effective field which is composed of repulsion between individual ions and any residual vertical field due to misalignment of the grid assembly, and nearby ground potentials.

This field is effectively constant for the curves shown in Figs. 3 and 4. The collector is of finite height (~ 2 cm) and thus an ion takes a characteristic time t to go beyond the collector's range. We get, therefore, a cross section of the form $\sigma=\sigma_0\exp(-pt)$, where σ_0 is the cross section below the "lifetime edge." As was pointed out previously, the only unknown in p is the ion radius R, so we may find R by fitting σ to the experimental curves. This procedure is complicated by the fact that t is also unknown, as is its dependence on temperature and pressure.

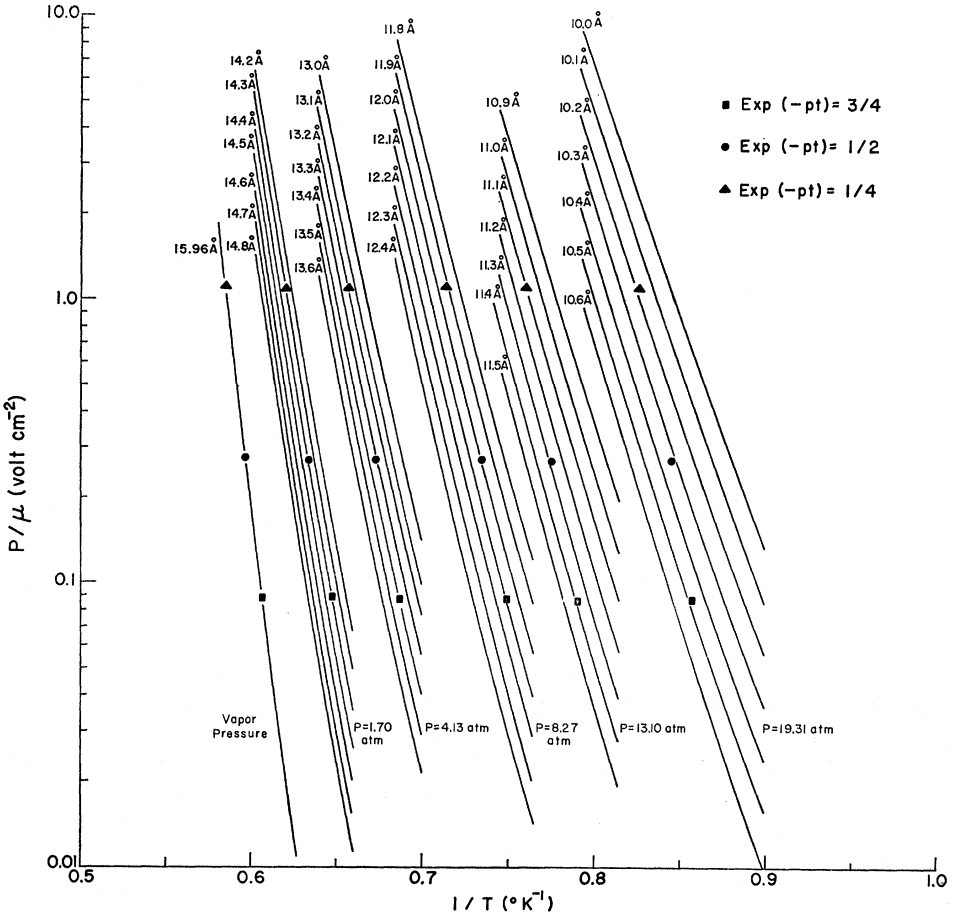

FIG. 6. Examples of the procedure outlined in Sec. III for obtaining R for several values of $\exp(-pt)$ with $t \propto 1/\mu_-$.

Douglass[6] has measured directly the mean lifetime at the vapor pressure, and Parks and Donnelly[19] have found that $R=15.96\pm0.04$ Å best fits those measurements; Tanner[18] also finds that this value of R fits his vapor-pressure cross-section measurements well over the lifetime edge. Accordingly, we take the value of the radius at the vapor pressure as known. This allows us to find t at the vapor pressure since we may calculate p and we have measured σ. At any other pressure and temperature, t will be different and depends inversely on the mobility of the trapped ion along a line. It is known[6,20] that this mobility is less than that of the free ion. Therefore, two assumptions may be made about the behavior of t which will give upper and lower limits on the actual time t: (a) Assume that t remains constant throughout; (b) make t vary inversely as the free-ion mobility. The sequence of operations which was followed in deriving R was

(i) to find the P, T coordinates of points such that $\exp(-pt)=\frac{1}{2}$,

(ii) to calculate p according to the formulas of Appendix A,

(iii) to apply one of the two assumptions concerning t,

(iv) to plot p or p/μ_- against $1/T$ for various radii at the appropriate pressure, and

(v) to read off the value of ion radius at each pressure. An explicit example of this procedure is demonstrated by Fig. 6. Of course, one may choose values of $\exp(-pt)$ other than $\frac{1}{2}$.[21]

The results of such calculations as described above are shown in Fig. 7, where R is plotted against P. The upper curve in this figure is based on the assumption that t is constant; the middle curve is based on the assumption that t varies as $1/\mu_-$. These curves imply that dV/dP is a decreasing function of pressure, which is one of the predictions of the bubble model.

There remains one other quantity that changes with pressure. This quantity is the length over which ρ_s falls to zero at the core of the vortex. Near the core, ρ_s is given approximately[22] by $\rho_s r^2/(r^2+a^2)$. The length a has been taken as 1.46 Å in the above calculations, but

[19] P. E. Parks and R. J. Donnelly, Phys. Rev. Letters **16**, 45 (1966).
[20] J. J. Domingo (private communication).
[21] Figure 6 shows the effect of other choices.
[22] A. L. Fetter, Phys. Rev. **138**, 429 (1963).

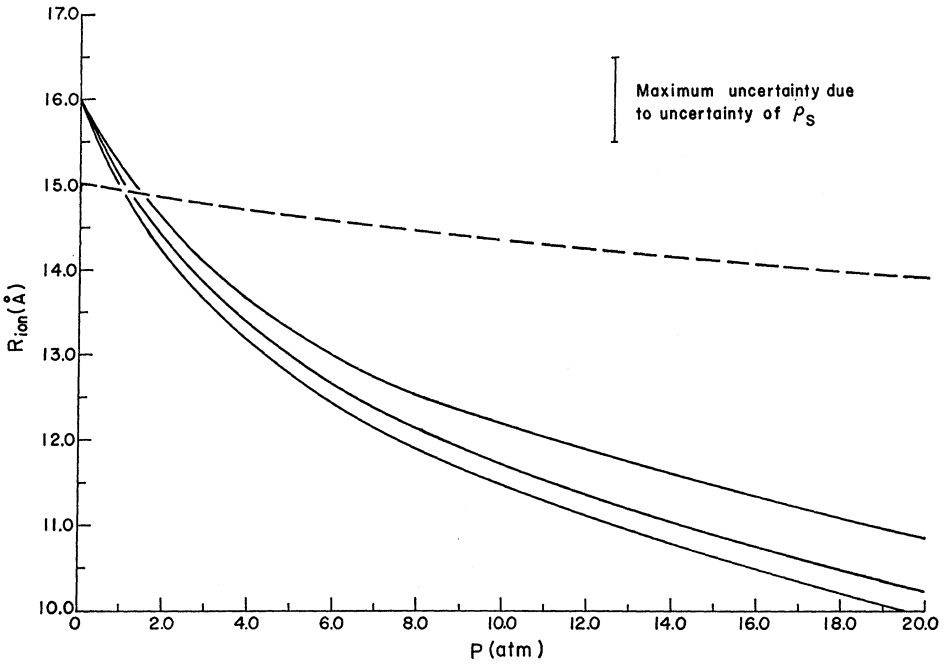

FIG. 7. Negative-ion radius as a function of pressure. The solid curves are explained in Sec. III. The dashed curve is based on the formula (Ref. 2) $R=15\times(8\pi a\rho_0)^{-1/2}$.

it depends on the square root of the fluid density. This variation has been taken into account in deriving the lower curve in Fig. 7. Shown in the upper right-hand corner of Fig. 7 is the maximum uncertainty due to the calculation of ρ_s. Thus we may conclude that the radius of the negative ion, as seen by a quantized vortex line, as the pressure is varied is given by the middle curve of Fig. 7 to an accuracy of $\pm 5\%$ at the highest pressures, and an accuracy of $\pm 3\%$ at low pressures.

IV. MOBILITY AS A FUNCTION OF PRESSURE

The mobility of the negative ion derived from Eq. (2) has been plotted in Fig. 8. The smoothed curves in this figure represent some 50 experimental points; the over-all accuracy of either curve is $\pm 1\frac{1}{2}\%$. The agreement at the vapor pressure with Meyer and Reif[3] is good, which means that our geometry is not causing the electric field to be much different from its nominal value. This was, in fact, checked independently by painting a replica of our geometry on carbon resistance board and plotting potentials in the drift region L. At the higher pressures, the curves of $\ln\mu_-$ versus P are straight lines with the limiting slopes -0.051 atm^{-1} at 1.025°K, and -0.042 atm^{-1} at 1.100°K. Assuming that only roton collisions are important at the temperatures in question,[3] one derives from the equations in Appendix B the following expressions for the slopes of Fig. 8:

$$[(1/P)\ln A(0)/A(P)-0.079]\,\text{atm}^{-1},\quad \text{at}\quad 1.025°\text{K}$$

and

$$[(1/P)\ln A(0)/A(P)-0.064]\,\text{atm}^{-1},\quad \text{at}\quad 1.100°\text{K},$$

where A is the ion-roton collision cross section and will be defined later. From the above two expressions and the measured values, one obtains

$$\ln A(0)/A(20)=0.48\pm 0.06;$$

the value obtained using radii taken from Fig. 7 is 0.65 ± 0.05. Thus we see that the internal consistency of the present experiments is quite good.

To be more explicit, we must have a theoretical estimate of the ionic mobility. At the temperatures and pressures we are considering, the roton-roton mean free path is at least of the order of the ion radius, so

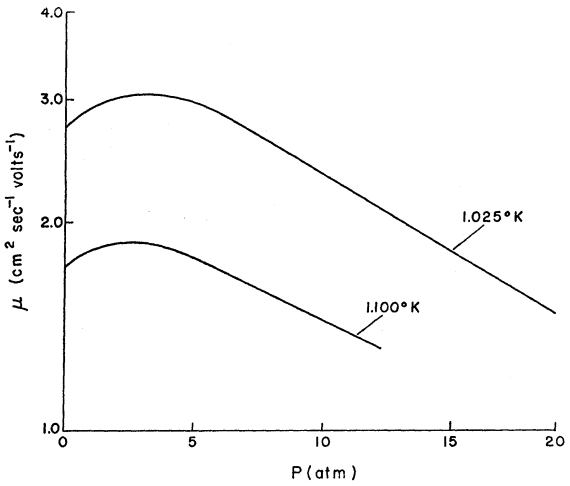

FIG. 8. Negative-ion mobility as a function of pressure. The positive-ion mobility does not exhibit a maximum and is a straight line within experimental error (Ref. 3).

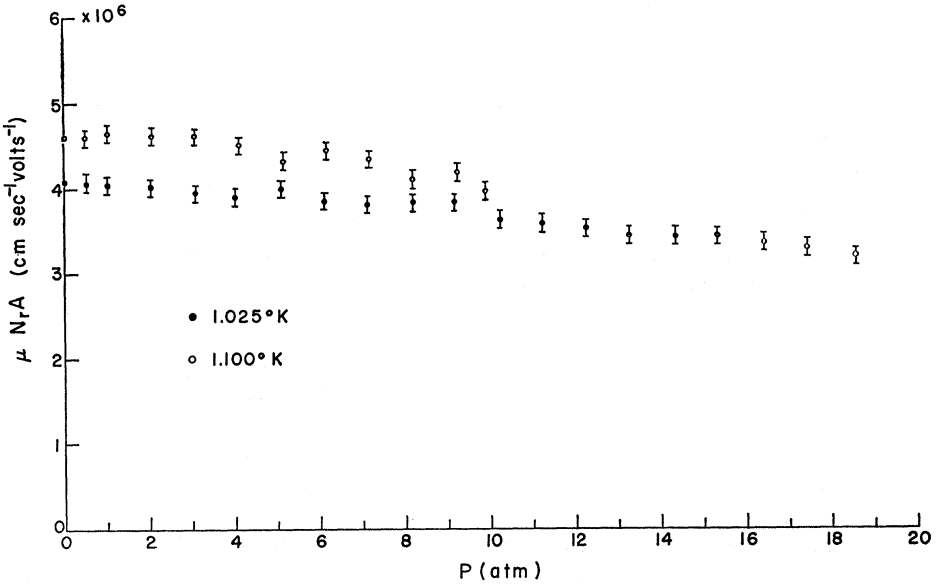

FIG. 9. ($\mu_- N_r A$) plotted against pressure, demonstrating that the maxima shown in Fig. 8 are due to changes in the ion radius.

that a Stokes-law mobility does not apply. The roton-roton mean free path is estimated from viscosity measurements; see, for example, Brewer and Edwards.[23] If we equate the gain of momentum per second from the field to the loss of momentum per second along the field direction due to ion-roton collisions, making allowance for persistence of velocity effects, we get for the ionic mobility

$$\mu_- = (e/2M)(\tau/f), \tag{4}$$

where τ^{-1} is the mean collision probability per second, f is the fraction of its momentum in the field direction that the ion loses in each collision, and M is the mass of the ion. Equation (4) may be rewritten as

$$\mu_- = (e/2M)(\lambda/fV). \tag{5}$$

Here λ is the ion-roton mean free path and may be written as

$$\lambda = [(N_i + N_r)A]^{-1}, \tag{6}$$

where

$$A = \pi(R + R_r)^2, \tag{7}$$

and

$$V = [V_i^2 + V_r^2]^{1/2} = [3kT/M + 2kT/\pi\mu_0]^{1/2} \tag{8}$$

is the mean relative thermal velocity between an ion and a roton. In the above expressions, (N_i, V_i) and (N_r, V_r) are the number density and thermal velocity of ions and rotons, respectively, R_r is the effective radius of a roton, estimated to be 4 Å by Landau and Khalatnikov,[24] and μ_0 is the roton effective mass as defined in Appendix B. For our conditions $N_i \sim 10^8$ cm^{-3} and $N_r \sim 10^{20}$ cm^{-3}, so that Eq. (6) becomes

$$\lambda = (N_r A)^{-1}.$$

If now we assume $M \sim 100\ m_{\mathrm{He}}$ (which is what most estimates of M give as an order of magnitude), $\frac{3}{2}\pi\mu_0 \ll M$, so that Eq. (8) reduces to

$$V = (2kT/\pi\mu_0)^{1/2}. \tag{9}$$

Substituting in (5) we get

$$\mu_- = (\pi/8)^{1/2}(e/Mf)(\lambda^2\mu_0/kT)^{1/2}. \tag{10}$$

There are, as yet, two unknowns in this equation, M and f. We do not expect f to change by more than a few percent as the pressure is varied. For the moment we will assume that M is a constant. Thus, if we plot ($\mu_- N_r A$) against P, it should have the same shape as a plot of $\mu_0^{1/2}$ against P. Such a plot is shown in Fig. 9 and it does, indeed, have a slight downward slope; from Appendix B this slope should be

$$[\mu_{0P}/\mu_{00}]^{1/2} = 0.79 = (N_r A \mu_-)_P/(N_r A \mu_-)_0. \tag{11}$$

Figure 9 gives for the right-hand side of this equation 0.77 ± 0.03. This result is good evidence that a gas kinetic picture gives a good starting point for examining ionic mobilities. Furthermore, it shows that the approximations we made in deriving Eq. (10) were reasonable ones, and, most importantly, that the assumption of constant mass for the ion is justified. It has been suggested[12] that the mass used for the ion in Eq. (10) should include its hydrodynamic mass, and that this mass is by far the larger part of its mass. Should this be true, M would vary as R^3; i.e., the value 0.79 quoted in Eq. (11) would be approximately 3.6, in total disagreement with the experimental value of 0.77. From

[23] D. F. Brewer and D. O. Edwards, in *Proceedings of the Eighth International Conference on Low-Temperature Physics, London, 1962*, edited by R. O. Davies (Butterworths Scientific Publications Ltd., London, 1963), p. 96.

[24] L. Landau and I. M. Khalatnikov, Zh. Eksperim. i Teor. Fiz. **19**, 637 (1949).

our measurements we are led to conclude that the negative ion has a large effective mass compared to μ_0, or, alternatively, $6M \gg m_{He}$, and that its hydrodynamic mass does not enter into the ion-roton scattering process. A further conclusion is that the product (Mf) is not very pressure sensitive.

V. THE BUBBLE MODEL

Much has now been written about this model for the negative ion.[12–16] The papers on the subject range from speculation to detailed calculation. The references quoted are only a sampling and have been chosen to show the progressive sophistication of the theoretical estimates of the ion radius, although the sophistication of a given model is no criterion for its applicability to the present experiments since it is possible to define the radius of the bubble rather arbitrarily. Experimentally we are dealing with an entity dynamically and it is to be assumed that both the electron and the helium atoms take part in the motion. Consequently, we shall adopt the rather simple approach of Ref. 16 and see how consistent are our radii with the model.

We start by noticing that the values that Burdick[25] obtained for the kinetic energy necessary to insert an excess electron into liquid helium can be derived to good accuracy from a Wigner-Seitz cell approximation. There results the equation

$$\tan k_0(c-a)=k_0 c \tag{12}$$

for the energy barrier, $V_0=\hbar^2k_0^2/2m_e$, that liquid helium presents to an electron. The electron–helium-atom scattering length a is given by $1.13(\hbar^2/m_e e^2)$,[26] and c is the distance between neighboring He atoms given by $\frac{4}{3}\pi c^3=1/\rho_0$. Our next approximation is to assume that the cavity created by the electron-helium repulsive interaction is characterized by the density distribution

$$\rho=0, \quad r<R,$$
$$\rho=\rho_0, \quad r\geq R,$$

i.e., that the electron is in a square well of depth V_0 and radius R. This, of course, ignores the details of the surface structure of the bubble, and in any refinement of the present model we must try to allow the surface of the bubble to be "soft." Hiroike *et al.*[15] have attempted this and find that the estimate of the radius given by Jortner *et al.*[14] is reduced somewhat. Here we shall adhere to the simple model and examine how much at variance with experiment is the assumption of a rigid wall. Cohen *et al.*[16] have shown that a rigid wall will be a good approximation provided that $(1-x^2)^{1/2}k_0 \ll \frac{1}{2}c$, where $x^2\hbar^2k_0^2/2m_e$ is the kinetic energy of the lowest state of the electron in its cavity. Table I shows some values of V_0, and E_e, the ground-state electron kinetic energy as a function of pressure. Also included are the experimental values of R from which the values are calculated. The value of V_0 at the vapor pressure, the calculation of V_0 by Burdick,[25] and the experimental values of Sommer[27] and of Woolf and Rayfield[28] are all within a few percent of each other.

TABLE I. Basic parameters of the bubble model.[a]

P(atm)	R(Å)	V_0(eV)	E_e(eV)
0	15.96	1.11	0.12
4.0	13.30	1.17	0.16
8.0	12.15	1.21	0.19
12.0	11.39	1.26	0.22
16.0	10.77	1.30	0.24
20.0	10.22	1.37	0.27

[a] $\mathcal{E}=20$ V/cm; $m_i=100m_{He}$

The total energy E_t of the bubble is composed of three terms: E_e, a surface energy E_s, and a pressure-volume term E_{PV}. Explicitly,

$$E_t=x^2\hbar^2k_0^2/2m_e+4\pi/3PR^3+E_s, \tag{13}$$

and the equilibrium radius is given by $\partial E_t/\partial R=0$, i.e.,

$$\partial E_s/\partial R=-4\pi PR^2-x\hbar^2k_0^2/m_e\partial x/\partial R. \tag{14}$$

The parameter x is given by the equation

$$x\cot(xk_0R)=-(1-x^2)^{1/2}, \tag{15}$$

and on evaluating $\partial x/\partial R$ and substituting in (14) we find

$$\partial E_s/\partial R=-4\pi PR^2+x^2(1-x^2)\hbar^2k_0^3 \times[k_0R(1-x^2)+(1-x^2)^{1/2}]^{-1}/m_e. \tag{16}$$

The left side of this equation is shown in the third column in Table II. As can be seen, it shows that E_s decreases as R decreases, but the picture is complicated by the fact that there is pressure and temperature variation associated with changes in R. Atkins and Narahara[29] have studied the surface tension of the free surface and find that it does not vary by more than 4% over the temperature range considered here. If we assume then that all the variation in E_s comes from

TABLE II. Variation of the surface energy of the bubble with R and P, the effective surface tension, and the expression (Ref. 33) $T=0.7\ hc\rho_0$. The ratio $(E_s+E_{PV})/E_e$ is 0.86±0.05 over the whole range.

P(atm)	R(Å)	$\partial E_s/\partial R$(dyn)	γ(dyn cm^{-1})	T(dyn cm^{-1})
0	15.96	2.3×10^{-6}	0.57	0.38
4.0	13.30	2.8×10^{-6}	0.85	0.44
8.0	12.15	3.2×10^{-6}	1.06	0.50
12.0	11.39	3.6×10^{-6}	1.27	0.55
16.0	10.77	4.2×10^{-6}	1.56	0.60
20.0	10.22	5.1×10^{-6}	1.97	0.65

[25] B. Burdick, Phys. Rev. Letters **14**, 11 (1965).
[26] T. F. O'Malley, L. Spruch, and L. Rosenberg, J. Math. Phys. **2**, 491 (1961).
[27] W. T. Sommer, Phys. Rev. Letters **12**, 271 (1964).
[28] M. A. Woolf and G. W. Rayfield, Phys. Rev. Letters **15**, 235 (1965).
[29] K. R. Atkins and Y. Narahara, Phys. Rev. **138**, A437 (1965).

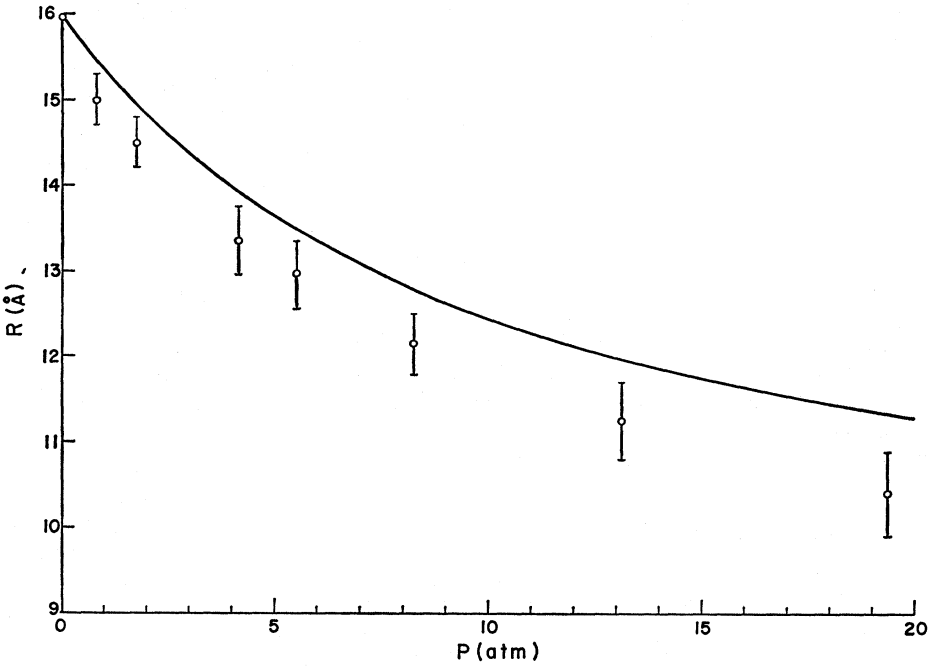

FIG. 10. Comparison of experimental points with a radius calculated using $\gamma=3.7879\rho$ dyn cm^{-1}.

structural changes in the surface of the bubble, we may write $E_s=4\pi\gamma R^2$, where γ is an effective surface tension. Then $\partial E_s/\partial R=8\pi\gamma R+4\pi R^2\partial\gamma/\partial R$ and the problem is now to try to dissociate changes in γ arising from changes in R and P. If we ignore $\partial\gamma/\partial R$, we can find a surface tension for sets of values of R and P. This is the quantity shown in column four of Table II. It shows a significant increase as P increases and R decreases which is reasonable since, physically, we would expect a stiffening of the surface of the bubble as it is shrunk. From the foregoing we can say that a slightly more sophisticated model of the bubble than that of a particle in a box[30] is not incompatible with the experimental data. A more complete evaluation of the negative ion on this basis must await further enumeration of some of the parameters involved by such experiments as are being conducted by Sanders *et al.*[31]

An alternative approach to the bubble has been made by Clark.[32] He uses a delta-function approximation to the helium-helium and helium-electron interactions and finds

$$R=15(8\pi a\rho_0)^{-1/2}. \tag{17}$$

This equation is plotted as the dashed line in Fig. 7. Using this same kind of model, Amit and Gross[33] find for the free-surface tension

$$T=0.7\hbar c\rho_0. \tag{18}$$

This is shown in the last column of Table II. The agreement of our data with this model is not too bad, especially since this model should only be at all valid for $T\sim 0$°K. An alternative comparison is shown in Fig. 10. Here (18) has been fitted to γ at the vapor pressure and γ made to vary as ρ_0. This gives the solid curve in Fig. 9. The experimental points obtained from Figs. 3 and 4 are also shown. The discrepancy is of the order of the radius of a He atom.

VI. POSITIVE-ION STUDIES

This section is a presentation of null results on positive ions and the conclusions to be drawn from them. First, no evidence of a trapping cross section was seen down to 1°K and up to a pressure of 20 atm. This indicates that the radius of the positive ion was always less than 9.0 Å in agreement with Ref. 19, and consequently it does not grow substantially with pressure. Presumably, one would have to be very close to the melting pressure before considerable growth occurred. Second, no change of mobility upon rotation was observed, in seeming contradiction to the results of Modena *et al.*[34] However, the small shift these workers observed may be explained by the fact that their current was fully space-charge limited and hence they were dealing with large cross sections and longer lifetimes. In the present instance, circumstances limited the applied field to 10 V cm^{-1} and the current was not space-charge limited.

[30] This model assumes a constant value for γ and an infinite potential well.

[31] For example, T. M. Sanders (private communication) has successfully excited the electron out of the bubble.

[32] R. C. Clark, Cryogenics **6**, 3 (1966).

[33] D. Amit and E. P. Gross, Phys. Rev. **145**, 130 (1966).

[34] I. Modena, A. Savoia, and F. Scaramuzzi, in *Proceedings of the Ninth International Conference on Low-Temperature Physics, Columbus, Ohio, 1964*, edited by J. G. Daunt, D. V. Edwards, F. J. Milford, and M. Yaqub (Plenum Press, Inc., New York, 1965), p. 342.

Finally, since at the higher pressures ($P \geqslant 12$ atm) μ_+ and μ_- behave in the same way, and since we have demonstrated that R_- can be measured, careful measurements of μ_+ and μ_- in this range should yield useful information on the relative differences between positive and negative ions.

VII. RELATION TO OTHER EXPERIMENTS

The experiments on vortex-ring creation and hot ions mentioned in the Introduction so far remain virtually unexplained. An interpretation of these experiments requires a knowledge of the size of positive and negative ions. One of the arguments put forward to explain the creation of ion-vortex complexes is that the velocity of an ion through the superfluid must exceed a critical value given by the velocity of the ring created, i.e.,

$$v_c = (\kappa/\pi R)(\ln 8R/a - 7/4).$$

To achieve a velocity sufficient to create a ring, an ion must reach v_c between collisions. There are two consequences of this. One, the decrease of the negative-ion radius as pressure is applied to it means that it is feasible for the ion to create rotons before it creates rings because v_c becomes greater than the Landau critical velocity,[35] i.e., of the order of Δ^*/p_0^*. Recently, Rayfield[36] has demonstrated that this process does in fact occur. The fact that such an effect does not occur for positive ions, in spite of their much smaller radius, cannot be so explained. To make this point clearer, Δ^*/p_0^* falls from about 60 msec^{-1} at the vapor pressure to about 45 msec^{-1} at 25 atm; v_{c-} runs from 54 to 74 msec^{-1} using our values for the radius; v_{c+}, using the value of R quoted by Parks and Donnelly, starts at 80 msec^{-1} and is still greater than 60 msec^{-1} if we use our value for the upper limit on R_+. Thus it is perfectly reasonable that negative ions should create rotons above a pressure of 12 atm as found by Rayfield, but the model fails to explain why positive ions create stable rings at all.

The second consequence of the model is that at higher temperatures, where it is known[9] that rings can be created by sufficiently high electric fields, the quantity $E_c(N_r A)^{-1}$ should be a constant. (E_c is the field necessary to create rings.) This means that a plot of $\ln E_c$ versus $1/T$ should be a straight line to first order with a slope Δ. This is what is found by Bruschi *et al.*[9] Here again it was found that the positive-ion behavior does not parallel that of the negative ion.

Domingo[20] has measured the mobility of a negative ion transmitted along a vortex line and in order to use such a technique for a study of the vortex line itself, the parameters of the ion need to be known. He finds that in this transmission process an extra scattering of the ion occurs, presumably because the ion is severely constrained in its motion by the vortex line. A study of this effect as a function of pressure hopefully would yield information about the structure of a vortex line. For instance, the Landau model indicates an increase of normal fluid density near the vortex core.

VIII. CONCLUSION

We have demonstrated that the radius of the negative ion may be measured to within 1 Å as a function of pressure by examining the escape of such an ion trapped by a quantized vortex line in rotating He II, that the pressure variation of the radius so found gives a semi-quantitative explanation of the pressure variation of the mobility of negative ions, and that the pressure variation is in accord with the bubble model for an electron in liquid helium.

It has been also pointed out that a knowledge of the radius of either sign of ion is necessary in attempting to interpret the process of vortex-ring creation and in evaluating theories of the ionic mobilities.

Finally, in order to obtain still more accurate values of radius, the probability of escape and the superfluid density must be measured directly and an attempt must be made to correct the escape calculation for any disturbance of the superfluid flow pattern caused by the ion, and any internal pressure variation at the vortex core.

ACKNOWLEDGMENTS

The author wishes to express his appreciation to Professor R. J. Donnelly for his continued encouragement and enthusiasm, and for his help in overcoming the many problems associated with the experimental hardware. Thanks are also due to Professor M. H. Cohen for illuminating discussions concerning the bubble model, P. E. Parks for his assistance with the details of the computation outlined in Appendix A, J. V. Radostitz and A. Dudiak for constructing the experimental apparatus and providing many helpful suggestions during its design, and R. W. Koster, who executed all the figures and greatly assisted in keeping the rotating cryostat rotating.

This work was submitted in partial fulfilment of the Ph.D. requirements of the University of Chicago.

APPENDIX A

The calculation of the probability of the escape of an ion from a vortex line as outlined in Ref. 19 is somewhat simplified when the ion is large, the applied electric field small, and the temperature above 1°K. In this Appendix, the simplified expressions for the quantities appearing in Eq. (3) will be written down and their physical significance stated briefly.

Under the conditions of the experiments we have

[35] See, for example, E. M. Lifshitz, *Helium* (Consultants Bureau, Inc., New York, 1959), Supplement.
[36] G. W. Rayfield, Phys. Rev. Letters **16**, 934 (1966).

TABLE III. Some typical values of the parameters defined in Appendix A.

R(Å)	P(atm)	T(°K)	ω_A(sec^{-1})[a]	ω_C(sec^{-1})[a]	U(°K)	p/μ_-(V cm^{-2})
16.0	0	1.7	2.09×10^{10}	3.55×10^{8}	43.54	3.76×10^{-1}
		1.6	2.17×10^{10}	3.50×10^{8}	47.08	9.00×10^{-2}
		1.5	2.23×10^{10}	3.47×10^{8}	49.69	2.34×10^{-4}
	12	1.4	2.34×10^{10}	3.41×10^{8}	54.95	5.65×10^{-7}
		1.3	2.39×10^{10}	3.39×10^{8}	57.14	5.29×10^{-9}
	20	1.2	2.46×10^{10}	3.36×10^{8}	60.48	8.76×10^{-12}
		1.1	2.49×10^{10}	3.35×10^{8}	62.02	2.16×10^{-14}
13.0	0	1.7	2.22×10^{10}	3.94×10^{8}	31.96	3.86×10^{2}
		1.6	2.30×10^{10}	3.89×10^{8}	34.56	2.54×10^{1}
		1.5	2.37×10^{10}	3.85×10^{8}	36.47	1.77
	12	1.4	2.49×10^{10}	3.79×10^{8}	40.34	2.17×10^{-2}
		1.3	2.54×10^{10}	3.76×10^{8}	41.95	7.10×10^{-4}
	20	1.2	2.61×10^{10}	3.73×10^{8}	44.40	6.49×10^{-6}
		1.1	2.64×10^{10}	3.71×10^{8}	45.53	7.79×10^{-8}
10.0	0	1.7	2.38×10^{10}	4.49×10^{8}	21.31	2.33×10^{5}
		1.6	2.47×10^{10}	4.43×10^{8}	23.04	3.89×10^{4}
		1.5	2.54×10^{10}	4.39×10^{8}	24.32	6.68×10^{3}
	12	1.4	2.67×10^{10}	4.32×10^{8}	26.90	3.66×10^{2}
		1.3	2.72×10^{10}	4.29×10^{8}	27.98	3.77×10^{1}
	20	1.4	2.80×10^{10}	4.25×10^{8}	29.62	1.66
		1.1	2.83×10^{10}	4.23×10^{8}	30.37	8.47×10^{-2}

[a] $\mathcal{E}=20$ V/cm; $m_i=100m_{\mathrm{He}}$

described, $\beta^2M\gg\omega_A^2$, ω_C^2 so that (3) simplifies immediately to

$$p=(\omega_A\omega_C/2\pi\beta M)(S_A/S_C)\exp(-U/kT). \quad \text{(A1)}$$

β is the drag force on an ion given by $e/\mu M$, and we notice that the ion mass cancels out to first order so that only an approximate value of the mass is necessary. In the calculations to be described, the mass M was taken as 100 m_{He}. Further, (A1) shows that we may calculate p/μ_- directly, so that an exact knowledge of the pressure variation of the mobility is unnecessary in order to derive the middle and lower curves of Fig. 7.

Figure 11 gives an idealization of the well the ion is trapped in. The frequencies in the problem ω_A, S_A, ω_C, S_C refer to the frequencies at points A and C in the x and y directions, respectively (the x direction being the direction of net motion of the ion). These frequencies are derived from the curvatures at A and C and are given by

$$\omega_A^2=(\partial^2U/\partial x^2)_A;\quad S_A^2=(\partial^2U/\partial y^2)_A$$

and

$$\omega_C^2=-(\partial^2U/\partial x^2)_C;\quad S_C^2=(\partial^2U/\partial y^2)_C.$$

In the present case these expressions become

$$\omega_A^2=S_A^2=\pi\rho_s(\hbar/m)^2\times[-1+(2+a^2/R^2)(1+a^2/R^2)^{-1/2}\times\sinh^{-1}(R/a)][R(1+a^2/R^2)]^{-1},$$

$$\omega_C^2=3S_C^2=4\pi\rho_s(\hbar/m)^2R^3/x_c^4,$$

where

$$x_c=R(4\pi\rho_s\hbar^2/3e\mathcal{E}m^2)^{1/3}.$$

Physically ω_A, S_A represent the frequency at which the ion comes up against the barrier; ω_C, S_C represent a tunneling probability per second.

The two depths in Fig. 10 are U_0, the depth of the well below the zero of energy, and U_C, the energy of the ion in the electric field taking the center of the vortex as origin. The first depth is given by

$$U_0=2\pi\rho_s(\hbar/m)^2R[1-(1+a^2/R^2)\sinh^{-1}(R/a)]$$

and is essentially the kinetic energy of the superfluid displaced by the ion. It is well to notice that this expression for U_0 assumes (a) no change in shape of the ion, or bubble, and (b) no "healing" behavior on the ion itself. That these assumptions do not represent serious deficiencies in the theory is shown in Ref. 19. They may, however, prove to be a more serious difficulty when theorizing about the transmission of an ion

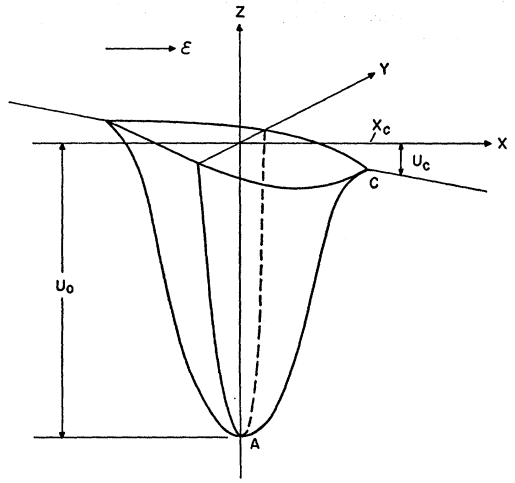

FIG. 11. Schematic representation of the potential well in which an ion is trapped by a quantized vortex line in the presence of an electric field.

along a vortex line. The second depth is given by

$$U_c = -2\pi\rho_s(\hbar/m)^2R^3/3x_c^2 - e\mathcal{E}x_c,$$

the two terms representing, respectively, contributions from the vortex and from the field. The total depth is given by

$$U_T = -U_0 + U_c.$$

The factor $\exp(-U/kT)$ is then just the Boltzmann distribution of ions in the well.

The calculation of the above quantities is quite cumbersome and was performed on a computer. Because it lies at the heart of the derivation of the ion radius from the data, a survey of the magnitudes of the quantities involved is presented in Table III.

APPENDIX B

The superfluid density ρ_s has been measured only at the vapor pressure.[37] It may be calculated at any temperature and pressure either from the Landau model or from thermodynamic variables. This Appendix describes a calculation of ρ_s using the Landau model. On this model one has the following expressions for the contribution to the normal fluid density of rotons and phonons, respectively:

$$\rho_r^* = \frac{2\mu_0^{*1/2}\hbar}{3(2\pi)^{5/2}(kT)^{1/2}}\left[\frac{p_0^*}{\hbar}\right]^4\left[1+6\hbar^{-2}\mu_0 kT\left(\frac{p_0}{\hbar}\right)^{-2}\right] \times\exp(-\Delta^* kT),$$

$$\rho_{ph} = 16\pi^5(kT)^4/45\hbar^3c_1^{*5}.$$

The asterisked quantities are those which vary with pressure and/or temperature. The neutron data of Yarnell *et al.*[38] and of Henshaw and Woods[11] yield the following values, where P is in atm:

$$\mu_0^* = 0.16(1-0.0217P)m_{He},$$
$$p_0^*/\hbar = 1.91(1+0.0029P)\ \text{Å}^{-1},$$
$$\Delta^* = 8.68(1-0.0084T^7)(1-0.0075P)^\circ\text{K},$$

where c_1^* is the velocity of first sound and its pressure and temperature variation are taken from Atkins and Stasior.[39]

The pressure coefficients in the above expressions are based on a linear interpolation of the neutron data. That this is a justifiable and quite accurate assumption may be seen from the results of Mills.[40] The same source justifies ignoring any temperature dependence of μ_0^* and p_0^*. The quantities ρ_r^* and ρ_{ph}^* were calculated on a computer and substituted in the expression

$$\rho_s = \rho^* - \rho_r^* - \rho_{ph}^*$$

to find ρ_s at any temperature and pressure. The values used of the total fluid density ρ^* were those of Keesom and Keesom.[41] The values of ρ_s found in this way agree to better than 2% with the measured values of Ref. 37. The thermodynamic calculation involves using four experimentally measured quantities. The expression for ρ_s in this case is

$$\rho_s = \rho^*\alpha^*/(1+\alpha^*);\quad \alpha^* = Cc_2^2/TS^2,$$

and calculations using the data of Maurer and Herlin[42] and of Lounasmaa and Kojo[43] give numbers that agree to within 10% of those calculated on the basis of the Landau model.

In the same manner one may calculate the roton and phonon number densities which are needed in the expressions for the negative-ion mobility.

[37] E. L. Andronikashvili, J. Phys. Moscow **10**, 201 (1946).
[38] J. L. Yarnell, G. P. Arnold, P. J. Bendt, and E. C. Kerr, Phys. Rev. **113**, 1379 (1959).
[39] K. R. Atkins and R. A. Stasior, Can. J. Phys. **31**, 1156 (1953).
[40] R. L. Mills, Ann. Phys. (N. Y.) **35**, 410 (1965).
[41] W. H. Keesom and A. P. Keesom, Leiden Commun. 224*d* (1933).
[42] R. D. Maurer and M. A. Herlin, Phys. Rev. **82**, 329 (1951).
[43] O. V. Lounesmaa and E. Kojo, Ann. Acad. Sci. Fennicae **A VI.36**, 3 (1959).